Investigation of first-passage-time problems in the two-mode dye laser

P. Lett
Department of Physics and Astronomy, University of Rochester, Rochester, New York 14627
(Received 31 March 1986)

The two-mode dye laser exhibits a quasibistable behavior wherein the lasing switches alternately between the modes at random intervals. This behavior can be described in terms of a first-passage-time (FPT) formalism. A Langevin model of the system has been the basis for most analytical approximations to the problem and here the results of detailed, four-dimensional, Monte Carlo simulations are presented. These results are compared to the various analytical and experimental results available. Attention is paid to the differences in alternative FPT problems and especially to problems involved in comparison with experimental data. One recent major advance in modeling the dye laser has been the introduction of pumping fluctuations into the Langevin equations. Effects of the introduction of pumping fluctuations on the FPT problem are explored and comments are made on previous attempts to account for their presence by the use of averaging techniques.

I. INTRODUCTION

A two-mode homogeneously broadened laser is a relatively simple system and yet presents an extremely rich spectrum of behavior to study. Investigations, both theoretical and experimental, of phase-transition analogies,[1-7] bistable behavior,[4-13] two-time intensity correlations,[7,14-18] first-passage-time problems,[4,19-26] and searches for deterministic chaos[27] have been reported based on this system. The relative simplicity of the Langevin approach to modeling the laser provides a theoretically tractable system of equations, while the presence of simple third-order nonlinearities lends a variety of interesting features to the dynamics of the system.

For the purpose of studying such bistable behavior in the context of a first-passage-time formalism and, in these studies, comparing theoretical and experimental results, the two-mode dye laser is one of the more convenient and popular systems. The experimental realization of this quasibistable laser system is relatively simple; in either single-frequency ring (two counterpropagating, traveling-wave modes) or standing-wave (two closely spaced longitudinal modes) configurations it will spontaneously switch between lasing in one mode (one direction in the ring laser) and the other. Measurements on both types of systems have been reported.[20,21]

The actual dye laser is, of course, a much more complicated system than the model would make apparent. It is, however, found that under certain conditions, specific forms of the Langevin description are very good models for the system. Several complications do arise, though, in attempting to extend the most basic of Langevin models to account for some of the observed behavior of the system. The basic two-mode, homogeneously broadened laser Langevin equations will manifest the fundamental features of the bistable behavior characteristic of the experimental system. It is found, however, that to adequately describe the detailed behavior of the system it is necessary to include fluctuations in the pump or gain terms of these equations as well as to keep the Langevin noise terms that represent spontaneous emission. This complication then produces a set of equations that, thus far at least, have proven analytically untractable.

In the following the first-passage-time problem will once again be examined. Results of a Monte Carlo computer simulation of the Langevin models will be presented with an emphasis on what effects the inclusion of pumping fluctuations have, and the results will be compared with the available experimental data.

In Sec. II we will briefly describe the analytic results available and the numerical methods used in this work. Before presenting any results relating to the first-passage-time problem itself it is helpful to have some familiarity with the system's overall behavior. In order to better understand the system a discussion of the general, qualitative behavior of the two-mode homogeneously broadened laser will be given in Sec. III.

The new results of this work will be presented in Secs. IV and V. The results of the simulations performed without pump fluctuations are presented first in Sec. IV and then the effects of their introduction are presented separately in Sec. V. Finally, general conclusions are reviewed in Sec. VI and the application of the results to other systems is discussed.

II. ANALYTICAL RESULTS AND NUMERICAL METHODS

The first-passage-time problem in the two-mode dye laser is investigated in some detail in Refs. 4 and 19–26, so only the most important and useful results from these works will be reproduced here. One of the simplest descriptions of the system is that of a pair of coupled third-order Lamb equations for the complex mode amplitudes, β_1 and β_2. Supplementing these equations with Langevin-type noise meant to represent spontaneous emission into the modes, we then have our starting point,

$$\dot{\beta}_1=[A_1-B(|\beta_1|^2-\xi|\beta_2|^2)]\beta_1+g_1(t)\ ,$$

$$\dot{\beta}_2=[A_2-B(|\beta_2|^2-\xi|\beta_1|^2)]\beta_2+g_2(t)\ ,$$

with

$$\langle g_i(t)g_j(t')\rangle = 4D\delta(t-t')\delta_{ij} .$$

We will work with a slightly simpler form of these equations. We introduce the dimensionless variables

$$E_i=(D/B)^{-1/4}\beta_i ,$$
$$t=(D/B)^{1/2}\tau ,$$
$$a_i=(DB)^{-1/2}A_i .$$

These substitutions uniquely scale both the saturation coefficient and the spontaneous-emission noise strength to unity. Thus we have

$$\begin{aligned}\dot{E}_1&=(a_1-|E_1|^2-\xi|E_2|^2)E_1+\tilde{q}_1(t) ,\\ \dot{E}_2&=(a_2-|E_2|^2-\xi|E_1|^2)E_2+\tilde{q}_2(t) ,\end{aligned} \tag{1}$$

where

$$E_1=x_1+ix_2,\quad \tilde{q}_1=q_1+iq_2 ,$$
$$E_2=x_3+ix_4,\quad \tilde{q}_2=q_3+iq_4 ,$$

and the coupling constant $\xi=2$ for a homogeneously broadened system. The spontaneous emission terms $q(t)$ are, again, taken to be δ-correlated white noise and are necessary to obtain the correct statistical behavior at low pump parameters but also to be able to see the switching behavior at all in the numerical simulations.[14,15] The pump parameters for the two modes can in general be different; however, for these investigations, we will always set $a_1=a_2=a$. We have then a system of four equations to implement on the computer or to solve analytically.

The inclusion of fluctuations into the pump parameter has been an important advance in modeling the intensity correlation functions of both the single-mode and two-mode dye lasers[14,15,28–34] and so we expect to see some effects of pumping fluctuations in the first-passage-time problem also. The equations, including pumping fluctuations, read

$$\begin{aligned}\dot{E}_1&=(a-|E_1|^2-\xi|E_2|^2)E_1+\eta(t)E_1+\tilde{q}_1(t) ,\\ \dot{E}_2&=(a-|E_2|^2-\xi|E_1|^2)E_2+\eta(t)E_2+\tilde{q}_2(t) ,\end{aligned} \tag{2}$$

with

$$\eta=\eta_1+i\eta_2$$

and the other symbols as above.

As is usual in these prolems we allow $\tilde{q}_1$ and $\tilde{q}_2$ to be δ-correlated white noise. Since the spontaneous emission is considered to take place on a time scale short with respect to the cavity-decay time this is considered a good approximation. The pump noise $\eta(t)$ is, however, taken as an exponentially correlated colored noise. Since it is derived from processes like turbulence in the dye flow it is not expected to take place on any particularly fast time scale and so the characteristic time is left as a free parameter $(1/\Gamma)$. The spontaneous emission terms q_i are independent of each other and their strengths have been scaled such that

$$\langle q_i(t)q_j(t+\tau)\rangle = 2\delta_{ij}\delta(\tau),\quad i,j=1,2,3,4 .$$

The colored-noise pump fluctuations have a strength given by another parameter Q. We have then, for the pump fluctuations,

$$\langle \eta^*(t)\eta(t+\tau)\rangle = Q\Gamma e^{-\Gamma|\tau|} .$$

$\eta(t)$ is an Uhlenbeck-Ornstein process for which the following equations can be written to describe its evolution:

$$\begin{aligned}&\dot{\eta}_i=-\Gamma\eta_i+\Gamma f_i(t),\quad i=1,2\\ &\langle f_i(t)f_j(t+\tau)\rangle = Q\delta_{ij}\delta(\tau),\quad i,j=1,2 .\end{aligned} \tag{3}$$

The model given by Eqs. (1) is the one upon which all analytic treatments of the first-passage-time problem have been based thus far. The model consisting of the six equations (2) and (3) is what is used in the numerical investigations in Sec. V with the effects of pump fluctuations included.

The numerical implementation of these equations is based on the work of Ref. 35. The method has been used elsewhere to study other problems associated with the laser with a noisy pump.[14,15,31,34] The equations are integrated for a small iteration time interval and a large number of iteration steps and this produces a record of the intensity of the two laser modes versus time, much like those measured experimentally.

Although the Eqs. (1) for the laser are four dimensional the phase space for the system is essentially two dimensional. That is, the distribution is uniform in the phases of the two fields and the only structure is in the two intensity dimensions. For a system of Langevin equations such as these there exists a corresponding Fokker-Planck equation for the probability density describing the system, $P(E_1,E_2,t)$. In this particular case the drift vectors satisfy what are known as the potential conditions and the steady-state probability density can be written as[21]

$$P(\mathbf{x})=Ne^{-V(\mathbf{x})}=Ne^{-V(I_1,I_2)} , \tag{4}$$

where

$$V(I_1,I_2)=\tfrac{1}{2}a(I_1+I_2)-\tfrac{1}{4}(I_1^2+I_2^2)-\tfrac{1}{2}\xi I_1I_2 . \tag{5}$$

The representative point for the system can be described as sitting on the "potential" surface V which, again, reduces to two dimensions for this problem.

The potential has two minima that lie near the points $I_1\approx a, I_2\approx 0$ and $I_1\approx 0, I_2\approx a$. The spontaneous emission is an additive noise which, in this case, can be described as jostling the representative point around on this potential surface. Eventually the system, if started in one well, will be pushed hard enough and in a proper direction so that the representative point scales the barrier and falls into the other well. The amount of time that the representative point requires to first pass beyond a certain boundary, given that it started within another, specified, region is known as the first-passage time for that particular trajectory (and that given set of boundaries). It is this quantity that will be investigated here.

The first-passage-time (FPT) problem for the potential given in Eq. (5) has been studied in the past using several different boundaries to define the problem. In Fig. 1 the two different first-passage boundary systems that have

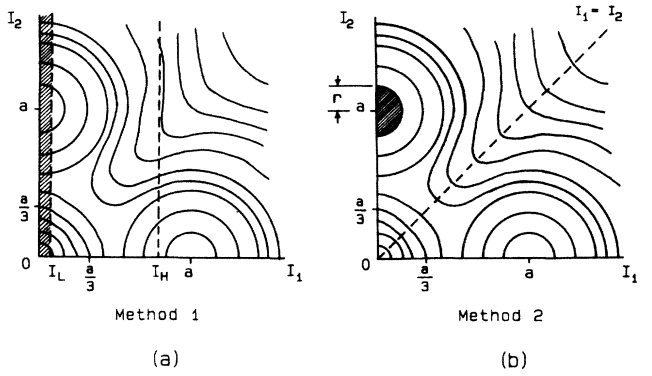

FIG. 1. Sketch of the FPT problems on the potential surface in the intensity phase space. Minima of the potential lie near the points $I_1=0, I_2=a$, and $I_1=a, I_2=0$ and there is a saddle point near $I_1=I_2=a/3$. (a) Method 1, a one-dimensional FPT problem is defined on the two-dimensional potential surface. The passage is defined as the time taken for a trajectory starting in the shaded region $I_1<I_L$ to cross the boundary $I_1=I_H$. (b) Method 2, a two-dimensional FPT problem starting from a semicircular region of radius r near one minimum of the potential and passing across the boundary $I_1=I_2$.

been the subject of much of the analytical work thus far are shown. In Fig. 1(a) a one-dimensional passage problem is indicated on a sketch of the potential surface. The system is assumed to start with one mode intensity in the region $I_1<I_L$ with a distribution that corresponds to the stationary distribution of the system (in one dimension) over that region. A first passage is deemed to have occurred when the representative point moves from its starting position in this region and passes, for the first time, past the boundary $I_1=I_H$. Since these boundaries are defined in terms of only one of the mode intensities (and calculations are done in one intensity variable) this is a one-dimensional FPT problem.

Since the system is not restricted to move in only one dimension a more accurate FPT problem will taken some account of the shape of the potential in the other dimensions. Method 2 [Fig. 1(b)] takes some account of this by taking the start region to be a half circle, radius r, centered on the deepest points of the wells, $I_1=a, I_2=0$ and $I_1=0, I_2=a$. A first passage is then considered across the boundary $I_1=I_2$ that separates the two wells. Estimates of the average first-passage times are not, then, directly comparable for the different methods and this should be borne in mind.

The inclusion of pump fluctuations into the system complicates the potential picture. First of all, the total phase space has been expanded by the addition of the noise variables. The system of equations (2) and (3) does not satisfy the potential conditions. Thus, the idea of picturing the system as a representative point in a two-dimensional phase space may no longer be mathematically accurate. Nonetheless, the FPT problem can be, and is, examined as a one- or two-dimensional problem, by ignoring the expanded phase space.

The first-passage times are extracted from records of intensity versus time like those shown in Fig. 2. The distribution of intensities from a long enough record (or many, shorter, ones) will be very close to the stationary distribution for the system. Extracting an average and a distribution of first-passage times from this record is straightforward. Although each passage trajectory is not independent of the rest as it would be in the ideal case, we find that estimates of various quantities pertaining to the two-mode dye laser problem are fairly accurate in spite of this admitted deficiency and at a substantial savings in computing time and costs. Although the Monte Carlo procedure used in Refs. 22 and 26 is much more statistically rigorous, in some ways much can be gained by looking at the system by the method used here.

In those references the equations are iterated until a passage is recorded. At this time the iteration procedure is stopped, new initial conditions are generated, and the iteration procedure begins again. In this way one does not have to rely on the convergence of the long-time average of the intensity distribution toward the stationary distribution as an ensemble average is produced with initial conditions already distributed according to the stationary distribution arrived at by analytic means. In addition, this reinitialization after a passage event insures that there is only a very small chance of getting overlapping trajectories included in the average. The resulting statistical independence of all of the trajectories makes error estimation straightforward. With the present technique, on the other hand, one relies on the overlapping trajectories to contribute something to the FPT distributions in order that one might reduce the computation time considerably.

The advantage of being assured of having the correct (stationary) distribution of initial conditions is, of course, lost when the stationary distribution is not available in analytic form. This is indeed the situation that we are in in the case of the laser with pumping fluctuations. As there is no known stationary distribution for the intensity in this case we must rely on the ergodicity assumption (that the time average is equivalent to an ensemble average) to obtain the result. It appears that the time average actually need not be performed over too long an interval to reproduce such properties as the stationary moments and the autocorrelations and cross correlations in situations that can be checked analytically. It is with the knowledge that the ergodic assumption works in these cases that it was assumed to be valid for the extraction of the stationary FPT distributions also.

There is still a requirement to iterate the equations for a substantial length of time in order to acquire a reasonable estimate of the average dwell time; that is, a significant number of switches from one well to the next must occur. As the system becomes more and more stable at high pump parameters (the wells become deeper), this requirement becomes prohibitively time consuming.

Analytic expressions for the average first-passage time have been given by several authors along with asymptotic expressions for both the long- and short-time behavior of the FPT distributions. All of these results are derived for the system of equations (1). An expression for $\langle T_p \rangle$ was first given by Singh and Mandel in Ref. 19 and put in

simplified form in Refs. 20 and 21. For a Method 1 type of first passage they find

$$\langle T_p \rangle \approx C \frac{\exp(a^2/12)}{a^2} \tag{6}$$

with $C = \frac{3}{2}(\pi/3)^{1/2}$. This formula (6) has been obtained several times in different ways, although the prefactor C has not been consistent from one derivation to the next. Other results have been $C = 3(\pi/3)^{1/2}$ (Ref. 22) and $C = \pi$ (Ref. 4) from one-dimensional approaches and $C = 4\pi/3$ (Ref. 4) and $C = 9(\pi/3)^{1/2}$ (Ref. 23) from multidimensional approaches.

Using an eigenmode analysis, and the Method 1 problem Hioe and Singh[4] arrived at the following result:

$$\langle T_p \rangle = \frac{\sqrt{3\pi}}{(\sqrt{3}-1)} \frac{\exp\left[\dfrac{a^2(\sqrt{3}-1)^2}{3}\right]}{a^2} . \tag{7}$$

A path-integral approach has also recently been applied to

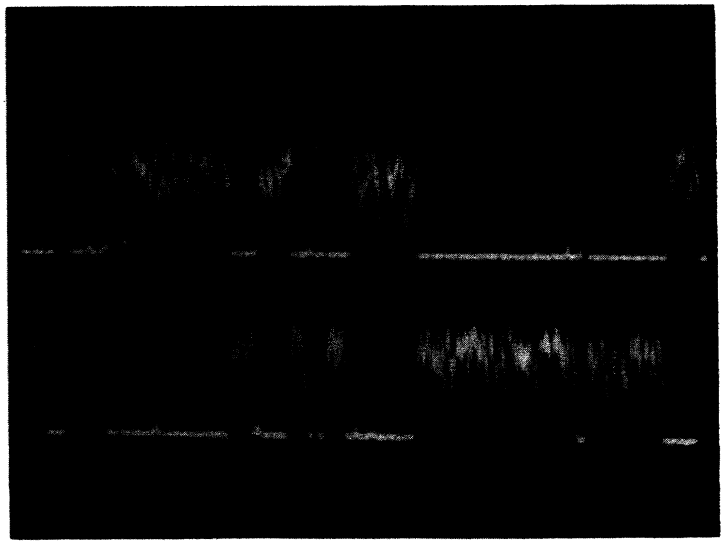

(a)

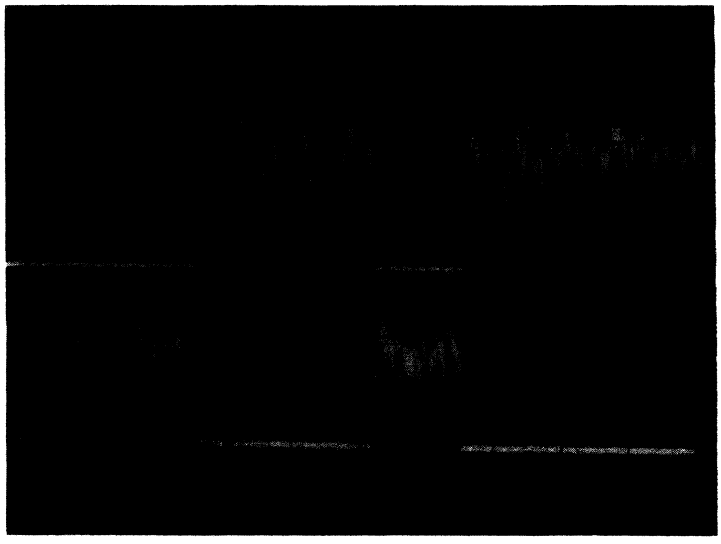

(b)

FIG. 2. Oscilloscope photographs of the mode intensities vs time for a two-mode dye ring laser. In each photograph the upper trace shows the time development of the clockwise propagating mode and the lower trace shows the counterpropagating mode. Spontaneous mode switching is evident in both cases. (a) represents laser operation at a slightly lower average pumping power than that in (b). In both (a) and (b) the traces shown are 0.1 sec in duration.

this problem[25] but this method does not yield any convenient analytical form for comparison here. There are no analytic results available for the system (2) and (3) with pumping fluctuations.

An asymptotic expression for the long-time behavior of the FPT distribution was first given in Ref. 20 for the Method 1 problem,

$$P(T_p)\sim\frac{1}{\langle T_p\rangle}\exp\left[-\frac{T_p}{\langle T_p\rangle}\right]. \tag{8}$$

This result has been derived again for Method 2 (Ref. 23)

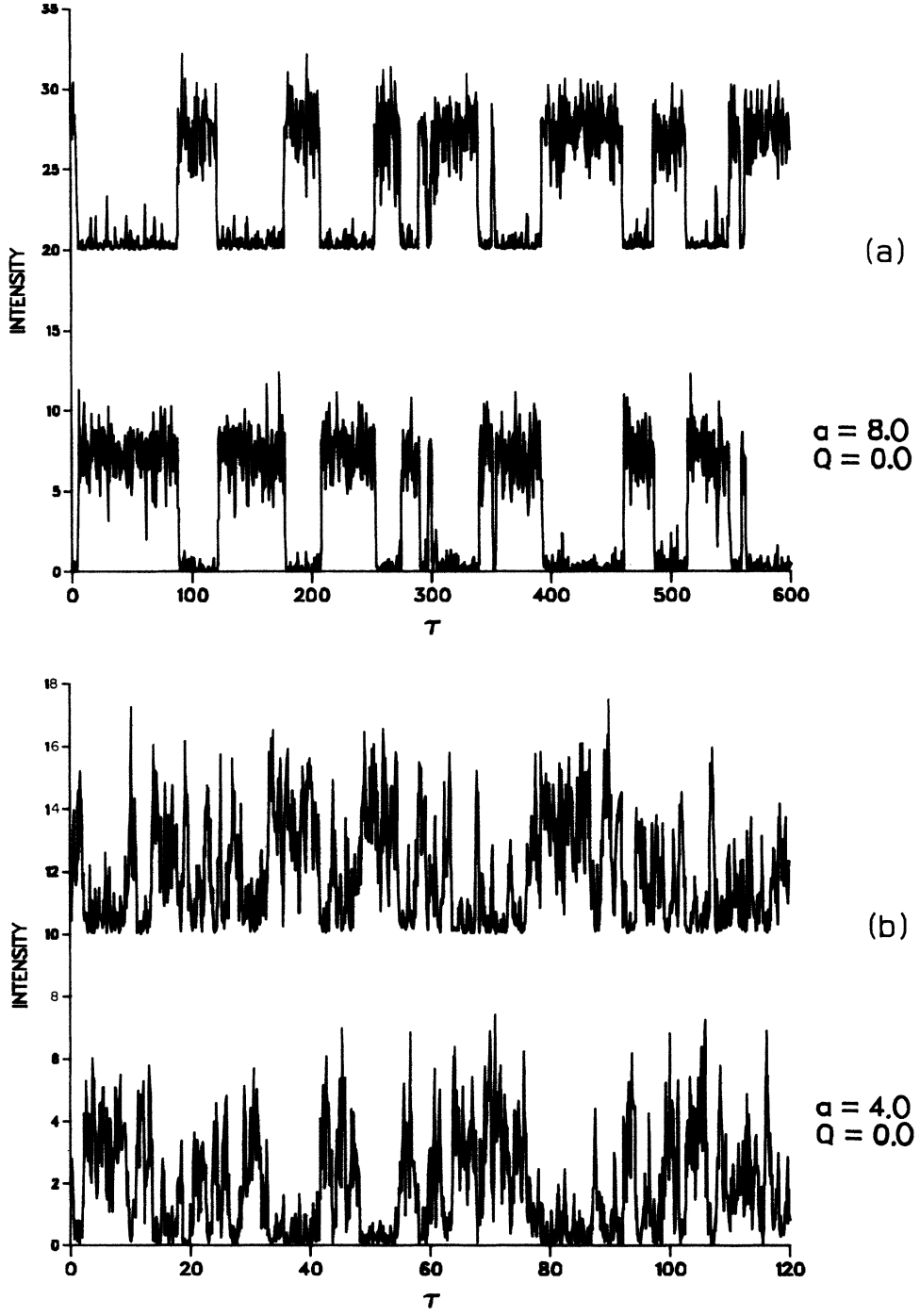

FIG. 3. Computer-generated Monte Carlo simulations of the intensity vs time behavior of the two-mode dye laser. (a) Simulation of Eqs. (1) with a pump parameter $a=8.0$ and no pumping fluctuations ($Q=0$). Mode 2 is offset by 20. (b) Simulation of Eqs. (1) with pump parameter $a=4.0$ and no pumping fluctuations. Mode 2 is offset by 10. (c) Simulations of Eqs. (2) and (3), including pumping fluctuations. Simulations were performed with a mean pump parameter $a=45.0$ and with pumping noise strength $Q=50$ and bandwidth of the pump fluctuations $\Gamma=100$. Mode 2 is offset by 200.

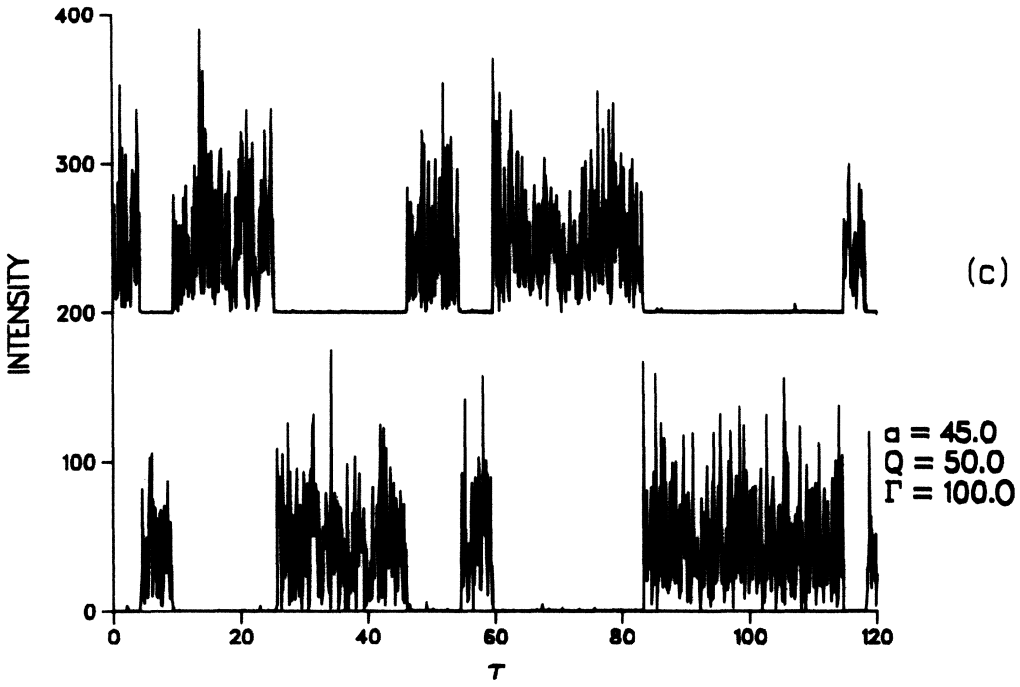

FIG. 3. (*Continued*).

but with a different expression for C used in the definition of $\langle T_p \rangle$. Lenstra and Singh have worked out a short-time asymptotic result for the Method 1 distributions. This rather complicated formula for the probability [Eq. (69) of Ref. 22] will not be reproduced here.

Given all of the various formulas for the average FPT and the FPT distributions, we must now note that, strictly speaking, neither of these two quantities have ever been measured and reported. The quantities measured in Ref. 20 were the *dwell time* distributions and their means. The relationship between these quantities can be somewhat complicated or quite simple, but they are not identical measures. A *dwell time* is measured as the time between the clear "switches," as seen in Fig. 2. In a one-dimensional Method 1 approach the *first-passage time* is concerned with one mode intensity. Instead of measuring from one switch event to the next, as in a dwell-time measurement, however, one now measures from any arbitrary point between two switch events to the next switch event.

In the case of the very clear switching of Fig. 2 there is little question that, to a very good approximation, for reasonably set passage boundaries, the average dwell time is twice the average first-passage time. Occasionally though, as the pump parameter is turned down, and especially under the influence of pumping fluctuations, the intensity of one mode may quickly cross the passage boundary and return; if one examines the intensity traces for the two modes no switch will appear to have occurred and yet a legitimate first-passage event, as defined above, has clearly occurred. This complicates the relationship between the average first-passage time and the average dwell time. Eventually, as the system behavior approaches that of Fig. 3(b) and the pump is turned down further still the dwell time is no longer very well defined. The FPT is, on the other hand, perfectly well defined whether the system is (quasi-) bistable or not. The relationship between the average FPT and average dwell time degrades, then, with decreasing pump parameter.

Given this complicated relationship between the averages of the two quantities it is even harder to see what the relationship is between their distributions. Again, the dwell-time distributions have been measured and compared to calculated FPT distributions and the validity of this procedure is open to some question. FPT distributions will be presented below and their features compared to those of measured dwell-time distributions without any claim to the validity of the assumption of a simple relationship being made.

III. OVERVIEW OF THE DYE LASER BEHAVIOR

Before discussing the first-passage-time problem any further the behavior of the two-mode dye laser will be reviewed in broad terms. The laser, without further coupling of the modes by such means as backscattering, is bistable—or at least quasibistable since it will switch states, from clockwise propagating to counterclockwise propagating, at random. This switching behavior is shown in the oscilloscope photographs of Fig. 2. The intensity of each of the output beams is displayed and the very rapid switching transitions are obvious.

Using the numerical method mentioned in Sec. II to integrate the equations of motion it is quite easy to produce a similar intensity-versus-time picture for a well-defined set of conditions represented by either Eqs. (1) or (2) and (3). In Fig. 3(a) we see such a trace produced by simulations done for a pump parameter $a=8$ and without pumping fluctuations ($Q=0$). Here again the rapid

switching behavior from clockwise to counterclockwise propagation is evident. The time scale of the simulation is in the dimensionless units defined by the equations above. We find that as the pump is turned down the behavior of the mode intensities becomes more and more erratic and the clear switching of the laser disappears.[14] In Fig. 3(b) we can see that the switching is essentially lost at a pump parameter $a=4$.

Figure 3(c) shows an intensity-versus-time plot with pumping fluctuations for the choice of $a=45$, $Q=50$, $\Gamma=100$. Comparing Figs. 2, 3(a), and 3(c) it is clear that the experimental intensity traces of Fig. 2 more closely resemble the computer solutions in Fig. 3(c) than those in Fig. 3(a). The one obvious effect of the introduction of pump noise is the suppression of the intensity noise in the mode that is "off," or not lasing as strongly. It is also obvious that when the mode switches back "on" the magnitude of the noise in that state is larger than it would be without the pump fluctuations. It is evident then that pumping fluctuations do significantly affect the operation of the actual laser system.

One condition should be placed on what has been said above about the introduction of pumping fluctuations. Only inasmuch as the fluctuations are fast with respect to time scales such as the intensity-correlation time or mean dwell time of the laser in one mode will they be able to produce the modifications in the intensity-versus-time behavior that are seen in the physical system. Obviously any very slow or "adiabatic" changes in the pump parameter (i) will not modify the behavior in the way the above fluctuations do but only raise and lower the mean dwell time in accordance with Eqs. (6) or (7) and (ii) can easily be eliminated from most experimental measurements.

This early conclusion leads to a comment on the use of convolution methods to incorporate pumping fluctuations. This method has been to average the results obtained, say for the mean dwell time or first-passage time, over a suitable range of pump parameters.[21,26] By convolving the analytic results for $\langle T_p \rangle$ given in Eqs. (6) or (7) with, say, a Gaussian spread function in the pump parameter a, pump drifts may be accounted for. These drifts, however, must occur on time scales slow enough so that the detailed behavior over the period of a few switches or so is unaffected. It is, after all, only then that Eqs. (6) and (7) for $\langle T_p \rangle$ are to be considered valid. As can be seen by the comparison of Figs. 2 and 3 this is not the case, and the pump fluctuations have to be dealt with more carefully.

A further point that is worth noting and that can be seen from looking at the intensity traces in Fig. 3 alone is that the range of parameters over which the first-passage-time problem can be treated here is somewhat limited. In the system without pump fluctuations, which is the system on which much of the analytic work has been done, it is seen that for pump parameters below about four or five the first-passage-time calculations are no longer comparable to the available experimental measurements which deal with dwell times rather than average first-passage times. Dwell times would be very difficult to extract from intensity traces such as those shown in Fig. 3(b).

IV. THE SYSTEM WITHOUT PUMP FLUCTUATIONS

The two-mode homogeneously broadened dye laser without pump fluctuations will be dealt with separately in this section, despite the importance of such fluctuations in practice. The reason is that there is a large body of existing analytic work that has dealt with just this problem. Thus it is a matter of some importance to compare these results, obtained using simulations of the full four-dimensional problem, to the analytic results obtained under various simplifying assumptions. The results for the system with the pumping fluctuations included will be examined in Sec. V.

The first matter to be examined will be the sensitivity of the average first-passage time $\langle T_p \rangle$ to the definition of the first passage and to the variation of the parameters involved. Figure 4 shows, for the case of $a=7.5$, the results of a numerical solution of Eqs. (1) giving the average first-passage time versus the boundary positions for the two different methods of defining the first passage.

In Method 1 (see Fig. 1) it is easily seen that $\langle T_p \rangle$ is relatively insensitive to the value of I_L as long as, say, $I_L < a/2$, so that the second well does not overlap the start region. Similarly, we find that $\langle T_p \rangle$ is relatively insensitive to I_H as long as $4 \leqq I_H \leqq 9$. As I_H moves above or below this range it either includes parts of the lower well of the effective one-dimensional potential, thereby increasing the chances of a very rapid passage and significantly lowering the mean, or it moves into an intensity region that is infrequently visited by the system, thus increasing $\langle T_p \rangle$ drastically. The former of these two cases will play an important role when the pump fluctuations are included in Sec. V.

In Method 2 we have only one parameter r, the radius

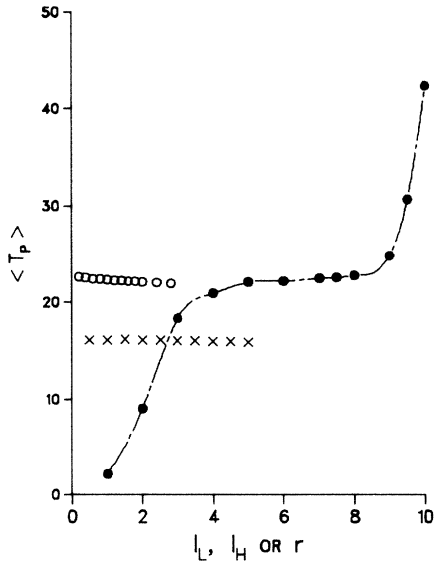

FIG. 4. Variation of the mean FPT $\langle T_p \rangle$ with the boundary parameters of the FPT problem. ○, $\langle T_p \rangle$ vs I_L for Method 1 (see Fig. 1); ●, $\langle T_p \rangle$ vs I_H for Method 1; and ×, $\langle T_p \rangle$ vs r for Method 2. The parameters $a=7.5$ and $Q=0$ (no pump fluctuations) were used.

of the initial well (region) in which we start the system. The crosses in Fig. 4 show the variation of $\langle T_p \rangle$ in Method 2 as a function of r. We see that as more points near the passage boundary are included $\langle T_p \rangle$ grows smaller but not significantly. $\langle T_p \rangle$ is again not very sensitive to variation of the boundary position.

Although each of these methods gives fairly robust results for the value of $\langle T_p \rangle$, the values actually obtained by using each of these methods do not agree. $\langle T_p \rangle$, as calculated by Method 1, is always somewhat larger than the same quantity calculated by Method 2.

Several of the analytic expressions for $\langle T_p \rangle$ given in Sec. II are displayed as a function of a, along with the numerical results obtained here, in Fig. 5. The values for the mean first-passage time, as determined by Method 1, are displayed as open boxes and those determined by Method 2 are indicated by solid circles. Analytic expressions representing Eq. (6) with the various prefactors (as explained in the figure caption) are also shown. It is obvious that, although the functional dependence on a is consistent among everything plotted, all of the predictions for the prefactor for Method 1 are too small by about a factor of 4. The results for Method 2, on the other hand, show that the theory of Ref. 23 predicts a value of $\langle T_p \rangle$ that is too large (although not by a large amount) when compared to the Monte Carlo results.[24]

Since Fig. 5 shows results from consideration of the system of equations (1), plotting $\langle T_p \rangle$ versus a is probably the most natural way of comparison, as a is the most easily accessible control parameter. On the other hand, when comparing theoretical predictions with experimental data, the most natural parameter to plot against is the mean intensity $\langle I \rangle$. Any plot of $\langle T_p \rangle$ versus a must otherwise assume some relationship between the measured quantity $\langle I \rangle$ and the plotted quantity a. Such a relationship is given in Ref. 36, but it was derived under the assumption of no pumping fluctuations.

Turning now to the probability distributions of the first-passage times, again one finds differences between those obtained by different methods and also differences as the parameters are varied. In Fig. 6 two plots of the probability density of first-passage times versus dimensionless time are shown, both created by computer solution of Eqs. (1) and using Method 1. Along with the Monte Carlo results plots of the long-time exponentials given in Eq. (8) are shown, using the value of $\langle T_p \rangle$ obtained from the simulations. Curves showing the behavior of the short-time asymptotic result of Eq. (69) of Ref. 22 are also drawn. The curves generated with the short-time asymptotic expression clearly do not fit the Monte Carlo distributions very well. The general form of

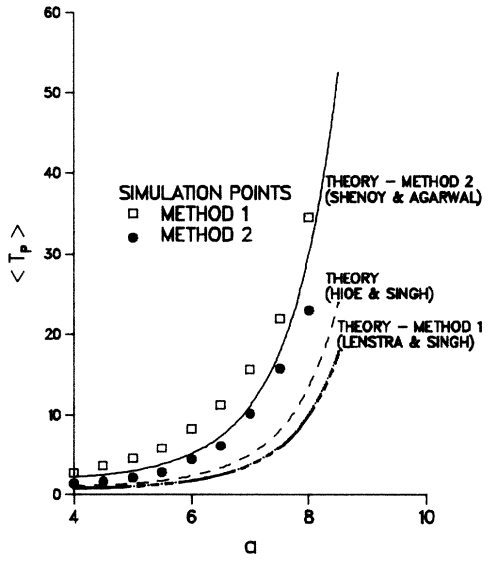

FIG. 5. $\langle T_p \rangle$ vs a for $Q=0$ (no pump fluctuations). □, simulation results using the Method 1 FPT problem. ●, simulation results using the Method 2 FPT problem. Theoretical curves are Eq. (6) with, from top to bottom, ——, $C=9(\pi/3)^{1/2}$ from Shenoy and Agarwal, Ref. 23, using Method 2. — — —, $C=4\pi/3$ from Hioe and Singh, Ref. 4, using a multidimensional approach akin to Method 2. · · · ·, $C=\pi$, again from Ref. 4, using Method 1 in a rotated coordinate system. Lying nearly on top of the last curve, —·—·, $C=3(\pi/3)^{1/2}$, from Lenstra and Singh, Ref. 22, using Method 1.

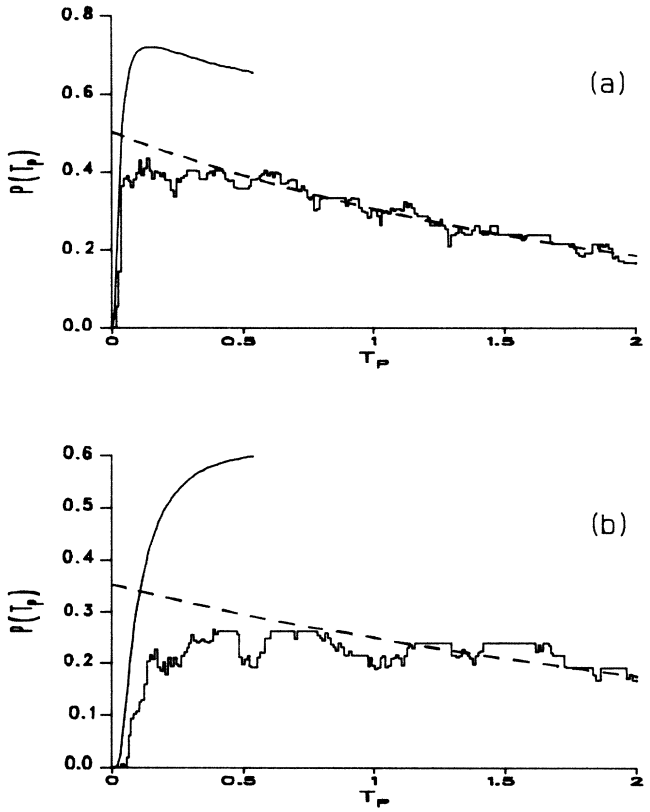

FIG. 6. Probability density of first passages vs first-passage time for pump parameter $a=6.0$ and no pumping fluctuations ($Q=0$). The histograms are produced by using Method 1 with (a) $I_L=1.0, I_H=2.0$ and (b) $I_L=1.0$, $I_H=3.0$. The solid curves are the short-time asymptotic expression [Eq. (69) of Ref. 22] and the dashed curves are the long-time asymptotic expression, Eq. (8), with the numerically extracted values of $\langle T_p \rangle$. In (a) $\langle T_p \rangle=1.99$ and in (b) $\langle T_p \rangle=2.83$.

the curves in Fig. 6, however, does appear to be correct even though the normalization of the curves does not. The short-time expression of Ref. 22 seems to assume a mean for the first-passage times that is much smaller than that actually found. (Indeed, this is also what was concluded from Fig. 5, above.) The analytic function rises up to meet what would be a much more rapidly falling long-time exponential than one actually finds. The long-time exponential form is certainly a good fit, provided that the numerically found value of $\langle T_p \rangle$ is used instead of the analytical predictions above.

Probability distributions generated by using Method 2 are shown in Figs. 7(a) and 7(b) with a pump parameter of eight and well radii of $r=0.5$ and 5.0. Here again the distribution rises from $P(0)=0$ and rapidly reaches the same long-time asymptote given in Eq. (8). As the radius of the well increases the initial rise of the distribution becomes much steeper, as evidenced in the figure. The increasing well radius includes more and more points closer and closer to the saddle point, and therefore many more short trajectories, to cause this rapid rise.

Figure 7(c) shows a distribution generated by Method 1 and using the same simulations as used to produce Figs. 7(a) and 7(b). The relatively slower rise of the distribution in Fig. 7(c) and the quickness with which the distributions reach the asymptote in 7(a) and 7(b) are evident. The average first-passage times are substantially different for the two methods as noted in the discussion above.

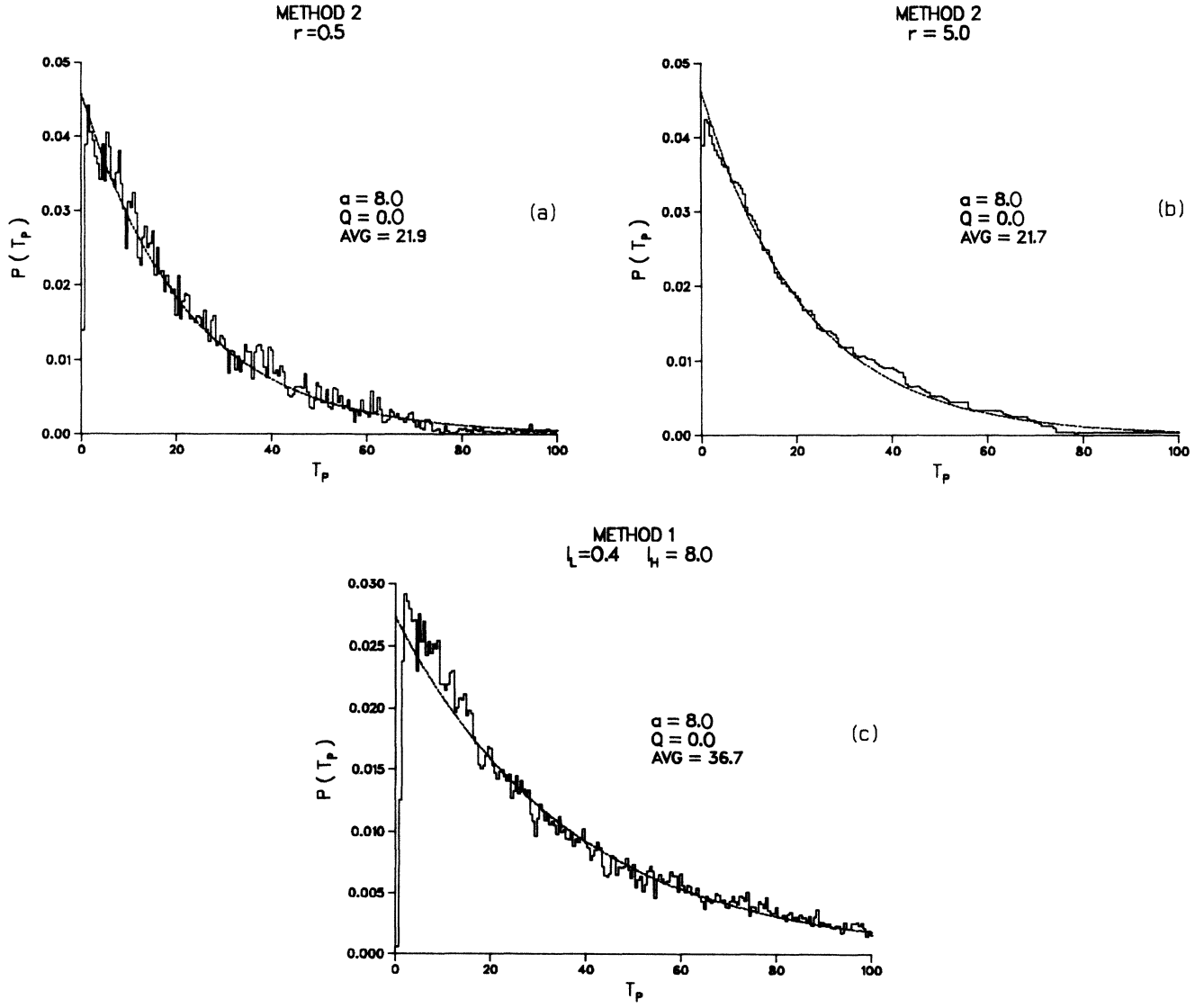

FIG. 7. Probability density of first passages vs first-passage time for pump parameter $a=8.0$ and no pumping fluctuations ($Q=0$). Histograms are the numerically extracted distributions and the smooth curves are the long-time asymptotic expression of Eq. (8) using the numerically extracted averages $\langle T_p \rangle$. (a) Distribution produced using Method 2 and $r=0.5$. (b) Distribution produced using Method 2 and $r=5.0$. (c) Distribution produced using Method 1 and $I_L=0.4$, $I_H=8.0$.

V. THE SYSTEM INCLUDING PUMP FLUCTUATIONS

The system of equations (2) and (3), with pump fluctuations included, was also investigated in the same manner as above. Many of the same comments may be made in this section as in the previous one except that in this case we must also specify the noise strength Q and bandwidth Γ of the colored-noise pump fluctuations in order to define the system. Recent studies have made it apparent that parameters $Q \approx 500$, $\Gamma \approx 1000$ may be more realistic than the values used here but this parameter change will only accentuate or moderate the effects discussed below. The important qualitative features have been confirmed.

In Fig. 8 the variation of the mean first-passage time with I_L, I_H, or r is shown for the case of $a=40$, $Q=500$, $\Gamma=5$. The crosses represent the variation of $\langle T_p \rangle$ with I_L and the boxes represent its variation with I_H in Method 1. $\langle T_p \rangle$ is, once again, relatively insensitive to their variation. One point to note is the wide range over which $\langle T_p \rangle$ is almost invariant with respect to variation of I_H in comparison with the small range for variation of I_L. It is apparent that the well shape is very much changed by the introduction of pump fluctuations. As might have been noted from observations made in Sec. III, the potential wells for the case with pumping fluctuations appear to be very long and narrow, stretched out along the intensity axes. The triangles in Fig. 8 show the variation of $\langle T_p \rangle$ with r in Method 2. It is, once again, only weakly varying and yields again consistently lower values for $\langle T_p \rangle$ than does Method 1.

With the introduction of pump noise into the system there are now three parameters on which $\langle T_p \rangle$ may depend. The variation of $\langle T_p \rangle$ with a still appears to be a rapidly rising function of pump parameter, whereas either shortening the correlation time of the noise or increasing the noise strength reduces $\langle T_p \rangle$. Both of these latter actions have the tendency to increase the excursions of the pump parameter from its mean value a.

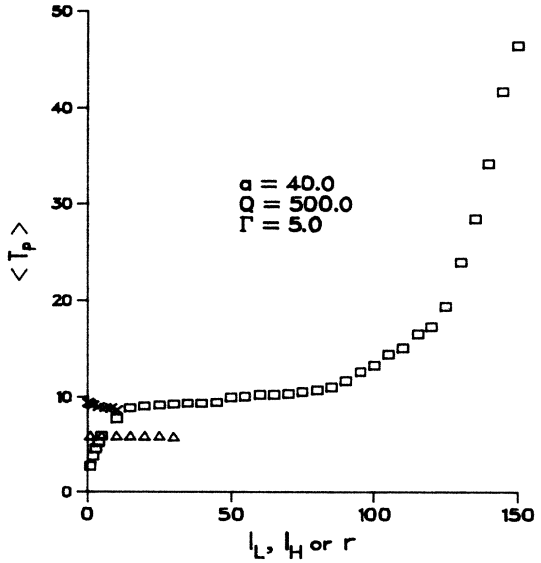

FIG. 8. Variation of the mean first-passage time $\langle T_p \rangle$ with the boundary parameters of the FPT problem under conditions of a fluctuating pump. $\times$, $\langle T_p \rangle$ vs I_L for Method 1. $\square$, $\langle T_p \rangle$ vs I_H for Method 1. $\triangle$ $\langle T_p \rangle$ vs r for Method 2. The average pump parameter $a=40.0$ and the strength and bandwidth of the pump fluctuations are $Q=500$, $\Gamma=5$.

From what has been said above it can be gathered that the rapid fluctuations in pumping due to dye-flow irregularities and the like are not likely to be well accounted for by the type of adiabatic convolution technique attempted previously. The effect of incorporating the pump fluctuations in the Langevin description of the problem on the variation of $\langle T_p \rangle$ with $\langle I \rangle$ is shown in Fig. 9. The original data of Ref. 20 are plotted versus mean intensity along with the analytic results of Eq. (6) (also plotted versus mean intensity by using the relationship given in Ref. 36). Also shown (as solid points) are simulation results including pump fluctuations characterized by the parameters $Q=50$ and $\Gamma=100$. In addition some new measurements, performed on a ring dye laser system, are presented for comparison in Fig. 9(b).

Plotting the dwell-time data and averaged FPT results versus mean intensity allows one to compare the two theoretical models on an equal footing. No assumptions are made about the relationship between the pump parameter and the mean intensity and each model is given its own scale factors for time and intensity to achieve a "best fit" to the data. In fitting curves to this data too much emphasis should not be placed on fitting points with extremely long dwell times. As pointed out by Roy *et al.*[20] originally, these points (with dwell times approaching a minute) are particularly sensitive to the effects of external perturbations. As mentioned in Sec. II the relationship of the average FPT to the average dwell time will be assumed to be a simple numerical factor of 0.5, and will be absorbed into the scaling constant for the time.

From Fig. 9 we can see that the average FPT as a function of $\langle I \rangle$ is not very sensitive to the introduction of the pumping fluctuations (although the scaling parameters do change). In comparison with the fluctuationless analytical formula, the convolution technique will produce a canted but more sharply curved function of a (or $\langle I \rangle$) than the fluctuationless analytical formula, as seen in Ref. 26. The introduction of the pump fluctuations into the Langevin equations, however, produces a less sharply curved function of $\langle T_p \rangle$ versus $\langle I \rangle$ than the fluctuationless expression. These simulation results, although they suffer from poor statistics, seem to fit the data better than do either of the other options. Another distinct advantage of the simulation results with the pump fluctuations included over the purely additive noise results is that the lowest intensity points are still consistent with the extraction of dwell times from the measurements of intensity versus time. The lowest point on the solid curves in Fig. 9 corresponds to $a=4$. This is certainly the limit for validity of Eq. (6) and a parameter that produces intensity traces resembling the one shown in Fig. 3(b). This would strain the abilities of any experimental system to extract dwell times.

The range of pump parameters used for the simulations in Fig. 9 was $10 \leq a \leq 50$ with the noise parameters $Q=50$

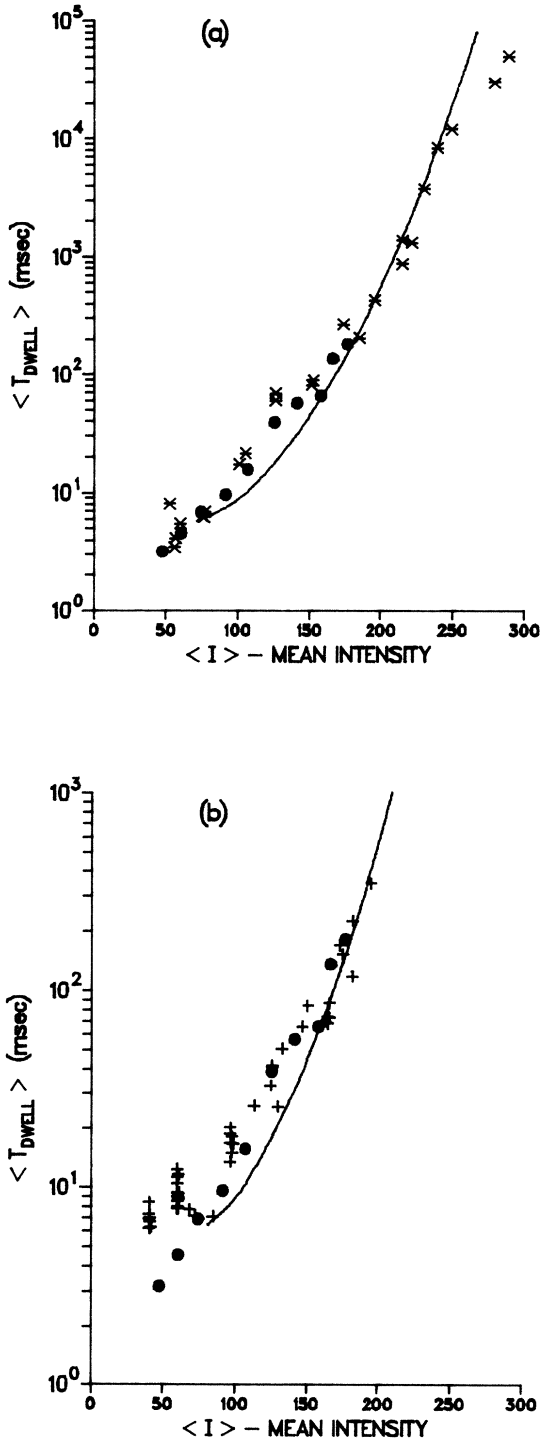

FIG. 9. Mean dwell time vs mean output intensity for a two-mode dye laser. In (a): ×, data from Ref. 20 taken using a two-mode standing wave dye laser. In (b): +, data taken using a two-mode dye ring laser. In both (a) and (b): ●, simulation results from Eqs. (2) and (3) with $Q=50$ and $\Gamma=100$ and pump parameter range $10 \leqq a \leqq 50$. ——, analytic expression, Eq. (6), derived assuming a constant pump ($Q=0$). In both (a) and (b) the scales are the experimental ones and the theoretical and numerical results include scale factors for both the dwell time and intensity for best fit.

and $\Gamma=100$. The average first-passage time was extracted by using Method 1 ($I_L=2.0, I_H=a$); however, the $\langle I \rangle$ dependence is the same for Method 2 and would simply imply a different scale constant for the dwell times. The range of intensities used in the simulations was limited, again, by the rapidly increasing dwell times and limited computing capacity.

The new data, shown in Fig. 9(b), are taken with a ring dye laser system. The fits of both the Monte Carlo calculations and the theoretical predictions without pump noise are much less satisfactory than those shown for the standing wave laser data in Fig. 9(a). The agreement could perhaps be improved somewhat over that shown by adjusting the time and intensity scale constants but the data in Fig. 9(b) definitely show a stronger dependence on $\langle I \rangle$ than the data in Fig. 9(a). Other ring laser data[21] have shown even more erratic behavior. The obvious difference between the ring laser and the standing wave laser is that, in the former, backscattering is present. This further couples the two modes and modifies the switching dynamics.

Finally, one can look at the influence of the pumping fluctuations on the distributions of first-passage times. The probability density of first-passage times along with the long-time asymptotic results of Eq. (8), generated by Methods 1 and 2, are shown in Figs. 10(a) and 10(b), respectively. Parameter values of $a=45$, $Q=50$, $\Gamma=100$ were used. The distribution for Method 2 in Fig. 10(b) shows very little qualitative difference from the distributions generated by Method 2 shown in Figs. 7(a) and 7(b). On the contrary, the distribution for Method 1, shown in Fig. 10(a), displays quite a striking new feature when compared to the Method 1 distributions in Figs. 5 and 7(c). A sharp peak that rises well above the asymptote and then falls sharply is now evident. The rise is exceedingly fast and not resolvable with this histogram bin size. Note that the ratio of I_L to I_H is about the same for Figs. 7(c) and 10(a) and that I_H is set approximately equal to the mean on-state intensity in each case. Reducing I_L by a factor of 10 begins to suppress this feature. The peak is due to the low-intensity region beginning to overlap the now-distorted potential well that lies along the axis of the mode intensity being examined. The FPT distribution now includes points that actually begin their trajectory in the well that one is "passing into" and thus contribute to the large number of very short passages that are seen in Fig. 10(a).

As the experimental data have all been taken under conditions something like Method 1, this feature may be expected to show up, in spite of the fact that these were dwell time and not FPT distributions, if pump fluctuations are truly important. A check of the results in Ref. 20 shows no such feature to be evident although the rather coarse binning of the distributions may hide a small peak just as it hides the initial zero in the distribution. The lack of a sharp peak in the distributions of Ref. 20 is, however, most likely due to the rather large integration time used in those measurements to facilitate distinguishing switch events from noise. The low-intensity excursions of the on state that produce this peak were precisely the noise that was being discriminated against. More recent measurements of dwell times[27,37] performed on a ring

laser system and using a minimum of integration have produced some additional (Method 1) data. A sample distribution is shown in Fig. 11. The sharp peak of Fig. 10(a) is clearly evident in Fig. 11 and is an interesting confirmation of the numerical work done here.

The presence, and the height with respect to the rest of the distribution, of the sharp initial peak is affected by several factors. The peak is enhanced by anything that enhances the magnitude of the excursions of the pump parameter from its mean. Thus either a larger strength Q or a shorter correlation time (larger Γ) for the pump noise would increase the peak height for a given mean dwell time of the system. (This assumes fixed passage boundaries with respect to the mean intensity.)

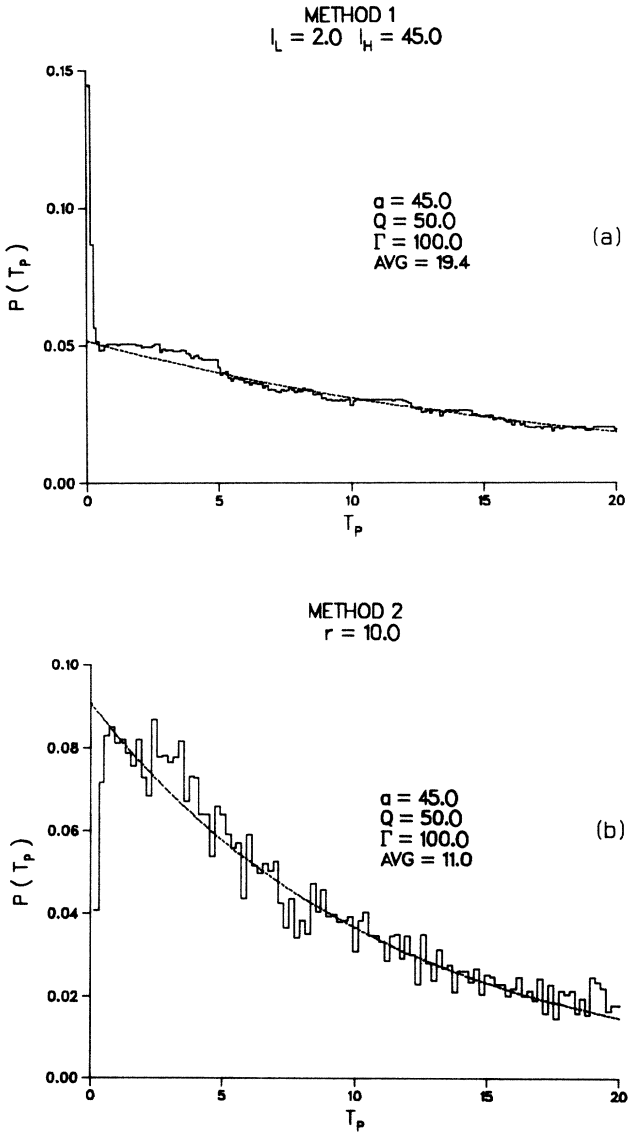

FIG. 10. Probability density of first passages vs first-passage time for a mean pump parameter $a=45.0$ and pump fluctuation strength $Q=50$ and bandwidth $\Gamma=100$. (a) Method 1 distribution: $I_L=2.0$, $I_H=45.0$, $\langle T_p \rangle = 19.4$. (b) Method 2 distribution: $r=10.0$, $\langle T_p \rangle = 11.0$.

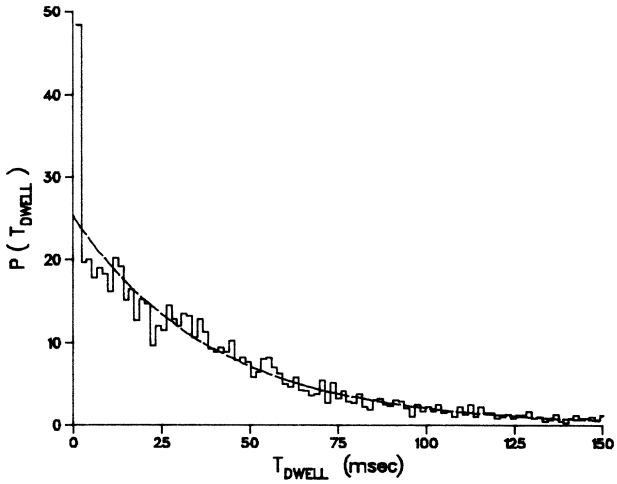

FIG. 11. Probability density of dwell times vs dwell time. The measurements were performed on a ring dye laser (from Ref. 27).

Lowering the pump parameter too far has the tendency to raise the initial point of the asymptotic exponential curve (accompanied by a faster decay) to the point where the sharp peak is no longer apparent. On the other hand, if the pump parameter is raised too far the fluctuations seldom reach the low-intensity barrier and the peak again recedes into the long-time exponential. The peak is most evident when $a \approx Q$.

Comparing the laser parameters, corresponding to Fig. 11, with the simulation parameters used in Fig. 10(a), we have $\Gamma_{\text{laser}} > \Gamma_{\text{sim}}$ and $Q_{\text{laser}} > Q_{\text{sim}}$. Integration in the experimental detection system would have reduced the peak height by an undetermined but probably substantial amount. The rest of the distribution decays away more quickly in Fig. 11 than in Fig. 10(a) because the experimental measurements were performed closer to "threshold" than the simulations.

VI. CONCLUSIONS

One of the fundamental problems in working with dye lasers near their operating threshold is that pumping fluctuations play a rather large role in modifying some aspects of their behavior. In order to study this system, including the fluctuating pump, a four-dimensional Langevin model was subjected to an extensive examination by Monte Carlo techniques.

An example of the interesting new features discovered in the FPT results due to the introduction of pumping fluctuations in the two-mode dye laser system is the sharp initial peak in the first-passage-time distributions, when calculated by Method 1. This peak was first discovered by numerical calculations and confirmed in recent experiments by Chyba *et al.*[27] The numerical investigations of the system allow one to easily see the variation of the mean first-passage time with various parameters and, most importantly, also allow one to remove the pump fluctuations from the system so as to provide a means of

testing the available analytic results. Since the pump fluctuations seem to be present in experimental systems and seem to affect the results substantially, the numerical work including a fluctuating pump also serves an important role as a predictive model for the actual system.

Although the finite time steps used in the numerical work may have a tendency to inflate the extracted values of $\langle T_p \rangle$ (see Ref. 22), the discrepancies between the analytic predictions and the Monte Carlo results are sufficiently large that they cannot be due solely to this. It is also worthy of note that the analytical results of Ref. 23 give estimates of $\langle T_p \rangle$ that are actually larger than the Monte Carlo results.

It can be seen from the foregoing discussion that some methods previously used to account for the presence of pumping fluctuations in the two-mode dye laser system are actually misleading. Attempts to fit the data have, in these cases, been made by incorporating the pump fluctuations into the calculations by an averaging method rather than by allowing the fluctuating control parameter to dynamically affect the system. This latter, more accurate, treatment leads to an immensely difficult analytic problem that is, however, readily amenable to numerical study as shown here.

Use of the averaging technique convolving the results for $\langle T_p \rangle$ with a spread function in a in Ref. 26 leads to some rather misleading conclusions. First of all the fit of the data to the analytic theory without pump fluctuations in the original Ref. 20 appears at least as satisfactory as that shown in Fig. 7 of Ref. 26. This is largely due to the method of fitting used in Ref. 26 (linear least squares on a log scale); this forces the curve through some of the most dubious of the points simply because they are the largest. In practice the long-dwell-time points are the most susceptible to outside disturbances and it is fairly clear from Ref. 20 that the two data points with the largest values of $\langle T_p \rangle$ are somewhat suspect. The inclusion of Monte Carlo results in the range $a < 4$ in a comparison with experimental *dwell times* is also misleading since the system is hardly switching in this region. This problem is present in both Refs. 20 and 26. This problem is eliminated by using a theory that incorporates the pump fluctuations into the Langevin equations of motion and thereby alters the pump parameter required to produce a given value of $\langle T_p \rangle$. A related but still more complex problem would be to include backscattering effects into the model.

A final observation is that the system that has always been identified with this type of work has been the two-mode dye laser. Although this system, especially in the single-frequency ring configuration, is an obvious choice for study there are other systems for which the same analysis holds. In particular, clear mode switching has been observed in two-mode semiconductor laser diodes.[38] These systems may indeed prove more suitable for this type of investigation, especially with regards to the control of pump noise properties. It is not clear whether or not these devices exhibit significant pump fluctuation effects or whether the significantly faster time scales of the switching will cause problems for the experimentalist.

ACKNOWLEDGMENTS

The author is deeply indebted to Professor L. Mandel for much guidance and encouragement and for helpful criticism at all stages of this work. Thanks are also due to T. Chyba and E. Gage for critical reading of the manuscript. This work was supported by the National Science Foundation and by the U.S. Office of Naval Research.

[1]R. Roy and L. Mandel, Opt. Commun. **23**, 306 (1977).
[2]R. Roy, Phys. Rev. A **20**, 2093 (1979).
[3]L. Mandel, Opt. Commun. **42**, 356 (1982).
[4]F. T. Hioe and S. Singh, Phys. Rev. A **24**, 2050 (1981).
[5]P. Lett, W. Christian, S. Singh, and L. Mandel, Phys. Rev. Lett. **47**, 1892 (1981).
[6]R. Roy and L. Mandel, Opt. Commun. **34**, 133 (1980).
[7]D. Kuhlke, Acta Phys. Pol. A **61**, 547 (1982).
[8]R. Roy and L. Mandel, Opt. Commun. **35**, 247 (1980).
[9]S. Schroter and D. Kuhlke, Opt. Quantum Electron. **13**, 247 (1981).
[10]D. Kuhlke and W. Dietel, Opt. Quantum Electron. **9**, 305 (1977).
[11]D. Kuhlke and G. Jetschke, Physica **106C**, 287 (1981).
[12]L. S. Kornienko, N. V. Kravtsov, and A. N. Shelaev, Opt. Spektrosk. **35**, 775 (1973) [Opt. Spectrosc. **35**, 449 (1973)].
[13]E. L. Klochan, L. S. Kornienko, N. V. Kravtsov, E. G. Lariontsev, and A. N. Shelaev, Zh. Eksp. Teor. Fiz. **65**, 1344 (1973) [Sov. Phys.—JETP **38**, 669 (1974)].
[14]P. Lett and L. Mandel, J. Opt. Soc. Am. B **2**, 1615 (1985).
[15]P. Lett and L. Mandel, in *Coherence and Quantum Optics V,* edited by L. Mandel and E. Wolf (Plenum, New York, 1984), p. 157.
[16]F. T. Hioe, S. Singh, and L. Mandel, Phys. Rev. A **19**, 2036 (1979).
[17]D. Kuhlke and R. Horak, Opt. Quantum Electron. **11**, 485 (1979).
[18]D. Kuhlke and R. Horak, Physica **111C**, 111 (1981).
[19]S. Singh and L. Mandel, Phys. Rev. A **20**, 2459 (1979).
[20]R. Roy, R. Short, J. Durnin, and L. Mandel, Phys. Rev. Lett. **45**, 1486 (1980).
[21]L. Mandel, R. Roy, and S. Singh, in *Optical Bistability,* edited by C. M. Bowden, M. Ciftan and H. R. Robl (Plenum, New York, 1981), p. 127.
[22]D. Lenstra and S. Singh, Phys. Rev. A **28**, 2318 (1983); see also D. Lenstra and S. Singh, in *Coherence and Quantum Optics V,* edited by L. Mandel and E. Wolf (Plenum, New York, 1984), p. 165.
[23]S. R. Shenoy and G. S. Agarwal, Phys. Rev. A **29**, 1315 (1984).
[24]P. Lett and L. Mandel, in *Optical Instabilities,* edited by R. W. Boyd, M. G. Raymer, and L. M. Narducci (Cambridge University Press, Cambridge, 1986), p. 367.
[25]X. W. Wang, D. L. Lin, and F. T. Hioe, in *Optical Instabilities,* edited by R. W. Boyd, M. G. Raymer, and L. M. Narducci (Cambridge University Press, Cambridge, 1986), p. 383;

X. W. Wang and D. L. Lin, J. Phys. A (to be published).
[26]K. P. N. Murthy and S. Dattagupta, Phys. Rev. A **32**, 3481 (1985).
[27]T. H. Chyba, W. R. Christian, E. Gage, P. Lett, and L. Mandel, in *Optical Instabilities,* edited by R. W. Boyd, M. G. Raymer, and L. M. Narducci (Cambridge University Press, Cambridge, 1986), p. 253.
[28]R. Graham, M. Höhnerbach, and A. Schenzle, Phys. Rev. Lett. **48**, 1396 (1982).
[29]R. Short, L. Mandel, and R. Roy, Phys. Rev. Lett. **49**, 647 (1982).
[30]A. Schenzle and R. Graham, Phys. Lett. **98A**, 319 (1983); in *Coherence and Quantum Optics V,* edited by L. Mandel and E. Wolf (Plenum, New York, 1984), p. 131.
[31]P. Lett, R. Short, and L. Mandel, Phys. Rev. Lett. **52**, 341 (1984).
[32]K. Lindenberg, B. West, and E. Cortes, Appl. Phys. Lett. **44**, 175 (1984).
[33]R. F. Fox, G. E. James, and R. Roy, Phys. Rev. Lett. **52**, 1778 (1984); Phys. Rev. A **30**, 2482 (1984).
[34]S. N. Dixit and P. S. Sahni, Phys. Rev. Lett. **50**, 1273 (1983); in *Coherence and Quantum Optics V,* edited by L. Mandel and E. Wolf (Plenum, New York, 1984), p. 143.
[35]J. M. Sancho, M. San Miguel, S. L. Katz, and J. D. Gunton, Phys. Rev. A **26**, 1589 (1982).
[36]M. M-Tehrani and L. Mandel, Phys. Rev. A **17**, 677 (1978).
[37]P. Lett, E. Gage, and L. Mandel (unpublished).
[38]N. Chinone, T. Kuroda, T. Ohtoshi, and T. Kajimura, IEEE J. Quantum Electron. **21**, 1264 (1985); M. Ohtsu, Y. Otsuka, and Y. Teramachi, Appl. Phys. Lett. **46**, 108 (1985); M. Ohtsu, Y. Teramachi, Y. Otsuka, and A. Osaki, IEEE J. Quantum Electron. **22**, 535 (1986).

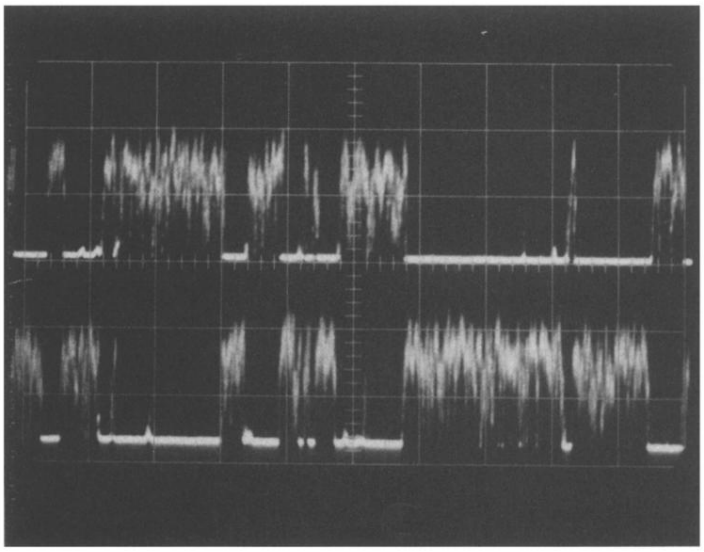

(a)

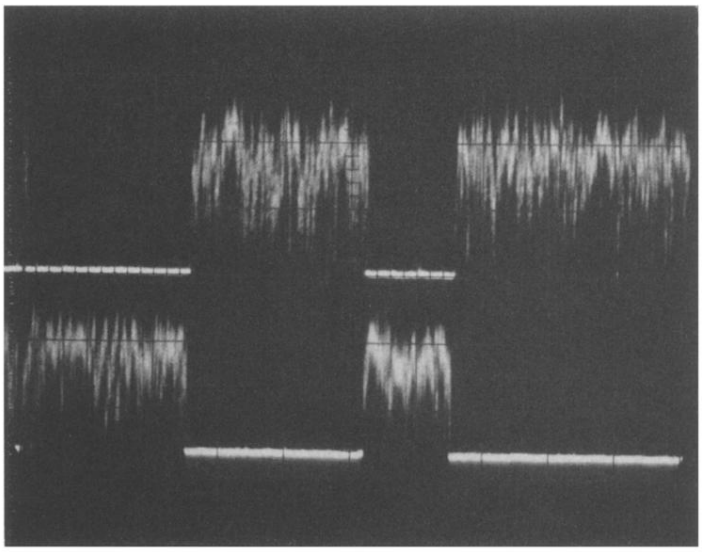

(b)

FIG. 2. Oscilloscope photographs of the mode intensities vs time for a two-mode dye ring laser. In each photograph the upper trace shows the time development of the clockwise propagating mode and the lower trace shows the counterpropagating mode. Spontaneous mode switching is evident in both cases. (a) represents laser operation at a slightly lower average pumping power than that in (b). In both (a) and (b) the traces shown are 0.1 sec in duration.